

# The Optimum Fins Length Distribution of Tabular PCM Heat Exchanger

Munther Mussa<sup>1</sup> and Hussein Hatem Saleh<sup>1</sup>

<sup>1</sup>University of Baghdad College of Engineering

October 9, 2023

## Abstract

The study aims to find the optimal fin length distribution for improved heat transfer during melting and solidification in a tubular PCM heat exchanger designed for heat storage. Three types of horizontal PCM tabular heat exchangers, all with five longitudinal fins, were studied numerically. While maintaining a constant heat transfer area, each model depicts a unique fin length distribution design. The first model, which serves as the reference design, has a homogeneous fin length distribution and each fin is 30 mm long. The second model has shorter upper and side fins and longer lower fins (20 mm for the upper fin, 25 mm for the side fins, and 40 mm for the lower fins). The third model has long lower fins but shorter than that of second model, short side fins and no change in upper fin length with reference design (30 mm for upper fin, 25 mm for side fins and 35 mm for lower fins). The findings indicate that the second model exhibits the best heat transfer performance for the melting process, while the first model is most effective for solidification. Interestingly, the third design emerges as the optimum choice for both melting and solidification processes.

## The Optimum Fins Length Distribution of Tabular PCM Heat Exchanger

Hussein Hatem Saleh <sup>a</sup>, Munther Abdullah Mussa<sup>a, \*</sup>

<sup>a</sup> Department of Mechanical Engineering, College of Engineering, University of Baghdad, 10071 Baghdad, Iraq.

\* Corresponding author.

**Abstract:** The study aims to find the optimal fin length distribution for improved heat transfer during melting and solidification in a tubular PCM heat exchanger designed for heat storage. Three types of horizontal PCM tabular heat exchangers, all with five longitudinal fins, were studied numerically. While maintaining a constant heat transfer area, each model depicts a unique fin length distribution design. The first model, which serves as the reference design, has a homogeneous fin length distribution and each fin is 30 mm long. The second model has shorter upper and side fins and longer lower fins (20 mm for the upper fin, 25 mm for the side fins, and 40 mm for the lower fins). The third model has long lower fins but shorter than that of second model, short side fins and no change in upper fin length with reference design (30 mm for upper fin, 25 mm for side fins and 35 mm for lower fins). The findings indicate that the second model exhibits the best heat transfer performance for the melting process, while the first model is most effective for solidification. Interestingly, the third design emerges as the optimum choice for both melting and solidification processes.

Key word: **PCM heat exchanger, melting, solidification, optimum, fin length distribution .**

**PCM** : phase change material

**H.E.:** heat exchanger

**H.T.F.** : heat transfer fluid

**CFD** : computational fluid dynamic

## Introduction

The increasing global demand for energy and the climate change crisis have compelled countries to embrace renewable energy sources such as wind and solar power. However, these energy sources are intermittent, meaning they cannot consistently generate energy when required. This mismatch between energy demand and the supply of renewable energy has been highlighted (Joudi and Taha 2023). Consequently, this has prompted the advancement of energy storage systems (Fathi and Mussa 2021).

Energy storage systems enable to store surplus energy generated during periods of high production, such as during sunny or windy weather, for later use when demand arises. Various storage solutions are in use, with the most prevalent being energy batteries, which find applications in electric vehicles and large-scale energy storage for power plants. Additionally, there are emerging technologies, including thermal and mechanical energy storage systems. Thermal energy storage involves the accumulation of excess thermal energy, often from solar collectors or other renewable sources, within materials capable of retaining heat energy. This stored thermal energy can be deployed as needed (Aneke and Wang 2016, Fathi and Mussa 2023).

Thermal energy storage can be accomplished using two primary methods: sensible heat storage and latent heat storage (Nabhan 2015). Among these, latent heat storage systems are particularly significant. These systems store heat within materials during phase changes, including processes such as melting, solidification, boiling, and condensation. In latent heat storage, energy is stored and released at a constant temperature. This characteristic enables stable energy charging and discharging, thanks to the consistent temperature difference between the phase change material (PCM) and its surroundings (Azim and Gupta 2020).

The applications of PCM storage systems include solar thermal energy storage, building heating and cooling systems, spacecraft PCM heat exchangers, and the use of PCM in human textile cooling systems, providing a comfortable and efficient way to manage body heat. All these applications used PCM inside heat exchanger (Nagar and Singh 2021).

PCM H. E. have shown significant potential in increasing energy efficiency and reducing the environmental impact of different thermal systems. One type of PCM H. E. that has received particular attention in recent years is the PCM fin heat exchanger, which consists of a PCM-filled fin that is attached to a heat transfer surface such as a tube or a plate (Al-Mudhafar, Nowakowski et al. 2018). The design and optimization of PCM fin H.E. pose several challenges, such as geometry, and phase change material, as well as the analysis of the heat transfer mechanisms and the evaluation of the performance metrics (Mehta, Vaghela et al. 2020).

Numerical investigation of horizontal fin PCM H.E. with longitudinal five fin, paraffin wax used as PCM due to high heat capacity, low melting temperature and chemically stable but low thermal conductivity, for this reason many research achieved to overcome this drawback (Al-Ebadi and Abdullah 2022, Sadiq and Mussa 2022), water used as heat transfer fluid H.T.F. due to high thermal conductivity and heat capacity. Geometry of PCM H.E. has a great effect on PCM H.E., the full understand of melting and solidification processes, where the natural convection is dominated mode of heat transfer, that depend in density change, and this natural convection up stream can restricted or enhance by geometry of container (Huang, Yang et al. 2022). So, the length of fin, fin density and fin angle are the main effects on PCM H.E., in addition of shape and orientation of PCM H.E., these parameters can enhance melting process but reduce solidification performance and vice versa (Motevali, Hasandust Rostami et al. 2021).

The selection of these parameters can be optimized to ensure the best performance of both the melting and solidification processes or to enhance one process over the other, depending on the purpose of the PCM heat exchangers (PCM H.E.) and the intended application. Emphasis should be placed on studying the fin length of tabular PCM heat exchangers. Specifically, examining the effects of different length distributions on the constant heat transfer area of the fin, and analyzing the heat transfer mechanisms within PCM heat exchangers with these length patterns.

Numerous studies have examined the impact of fin geometries on natural convection during the melting and solidification of phase change materials (PCM). For instance, (Rudonja, Komatina et al. 2016) investigated the enhancement of heat transfer in a shell and tube PCM heat exchanger designed for thermal energy storage. In this study, paraffin wax E53 was used as the PCM, and longitudinal rectangular copper fins were employed. A numerical analysis was conducted using a 3D model built in Ansys FLUENT software. The results demonstrated that increasing the ratio of heat transfer surfaces by raising the fin height led to a decrease in melting time. Furthermore, the study found that the number of longitudinal fins had a significant positive impact on melting time. Similarly, (Mehta, Chaudhari et al. 2017) studied the thermal performance of latent heat storage units filled with PCMs in various shell and tube configurations: vertical, horizontal, and inclined ( $45^\circ$ ). The investigation was carried out numerically using the enthalpy porosity approach. To reduce computational time, a 2D slice of the PCM heat exchanger was employed for modeling. It was observed from the results that the PCM melting process occurred more quickly in the inclined shell and tube configuration compared to the vertical and horizontal configurations. Additionally, the impact of varying fluid inlet temperatures on the thermal performance of the PCM heat exchanger was examined. The results indicated that higher fluid inlet temperatures led to a reduction in melting time. (Pizzolato, Sharma et al. 2017) studied a new method for heat transfer fins design for shell-and-tube heat exchanger used as thermal energy storage units, longitudinal fins are used. The topology optimization and multi-phase computational fluid dynamics used to design the optimal fin shape for a given PCM heat exchanger set of design constraints. The results demonstrated that the proposed method could identify fin shapes and designs that significantly improved the heat transfer performance of the PCM heat exchanger. In a separate study, (Kamkari and Groulx 2018) achieved experimental research to enhance the melting rate of PCM by adding fins to rectangular enclosures with different inclination angles. The findings revealed that the melting rate increased as the inclination angle decreased, both for unfinned and finned enclosures. Notably, in the case of a 3-fin horizontal enclosure, the minimum melting time was observed, resulting in the highest heat transfer rate. This study contributes to a better understanding of the PCM melting process in differently inclined finned enclosures and provides valuable benchmark data for future simulation studies. (Shahid Afridi, Anthony et al. 2018), did a comparative study, both experimentally and numerically, to evaluate the performance of annular and longitudinal fins in thermal energy storage units utilizing phase change materials (PCM). The results showed that longitudinal fins are more effective than annular fins for PCM storage units because it provides larger surface area of heat transfer, which contribute to higher heat transfer rate and higher efficiency. (Aydin, Mete et al. 2018) studied the effect of attaching a fin to the bottom of the inner tube in a horizontal shell-and-tube storage unit, that can enhance the melting rate process of paraffin that used as PCM by up to 72.8%. that because the fin intensifies the recirculation of melting paraffin or natural convection currents in the lower half of the annulus of sell side, that lead to increase the heat transfer rate. And the study suggested that fins can be an effective improvement to enhance the melting rate of paraffin wax in horizontal PCM shell-and-tube storage units, which may be useful for different applications such as thermal solar energy storage and building climate conditioning. (Deng, Nie et al. 2019) studied a novel fin arrangement was proposed to enhance heat transfer in latent heat thermal energy storage. Symmetrical fins were placed along the lower vertical centerline, improving melting significantly at specific angles. Effects of shell conductivity, dimensionless fin length, and heat-transfer fluid temperature were studied. Optimal angles reduced complete melting time by 66.7% with increased fin length and by 53.1% with higher fluid temperature. Longer fins exhibited more pronounced performance enhancement in latent heat thermal energy storage in this configuration. Similarly, (Mahood, Mahdi et al. 2020) conducted a numerical study to investigate the effect of fin height and angle in the performance of a horizontal shell-and-tube PCM heat exchanger. The results showed that increasing fin height significantly improved the thermal performance of the PCM heat exchanger, reducing melting time by 50% for a fin height equal to 0.8 of the hydraulic radius of the annulus shell. Additionally, the study found that lower fin angles, when positioned below the horizontal axis, provided better thermal performance by targeting the least efficient heat transfer region within the PCM inside the heat exchanger shell. Beyond fin shape, fin spacing and height were also found to impact the natural convection of melted PCM. (Soltani, Soltani et al. 2021) conducted a numerical investigation into the combined effects of fins and rotation on the melting and solidification processes of a latent heat thermal energy storage heat exchanger. Radial fins

were employed in a shell and tube PCM heat exchanger. The results demonstrated that rotational speed had a positive impact on both the melting and solidification processes, reducing the solidification process time by 83.21% and increasing the heat transfer rate by 12.89 W. Furthermore, an increase in rotational speed showed a direct correlation with the enhancement of the heat transfer rate by 2.45 and 3.87 times during the melting and solidification processes, respectively. In (Ali N. Abdul Ghafoor 2020) study LHTES with paraffin wax, circular tubes outperformed vertical and horizontal ovals, demonstrating superior efficiency and longer heat absorption duration.

Overall, these studies illustrated that, the addition of longitudinal fins can significantly enhance the thermal performance of PCM tubular H.E., and the optimum number and geometry of fins depend on the specific design and operating conditions of the heat exchanger.

The objective of this work to select the optimum design from three fin length distribution designs, the selected design, that gives heat transfer enhance for melting and solidification processes, by implemented numerical simulation of these designs in CFD and analyze the result obtained from simulation to conclude the optimum design.

### Mathematical and numerical model:

#### Mathematical model:

The typical heat exchanger (H.E.) problem is resolved by applying the heat diffusion equation, combined with continuity, momentum, and energy equations for steady-state conditions. In this context, each domain, whether solid or liquid, is addressed separately using the respective equations. However, the situation differs in the case of phase change material heat exchangers (PCM H.E.), where the melting and solidification processes change with time (transient), and the medium undergoes phase transitions during operation. The heat diffusion is transformed into an energy balance by include the PCM's enthalpy change during the phase change as following:

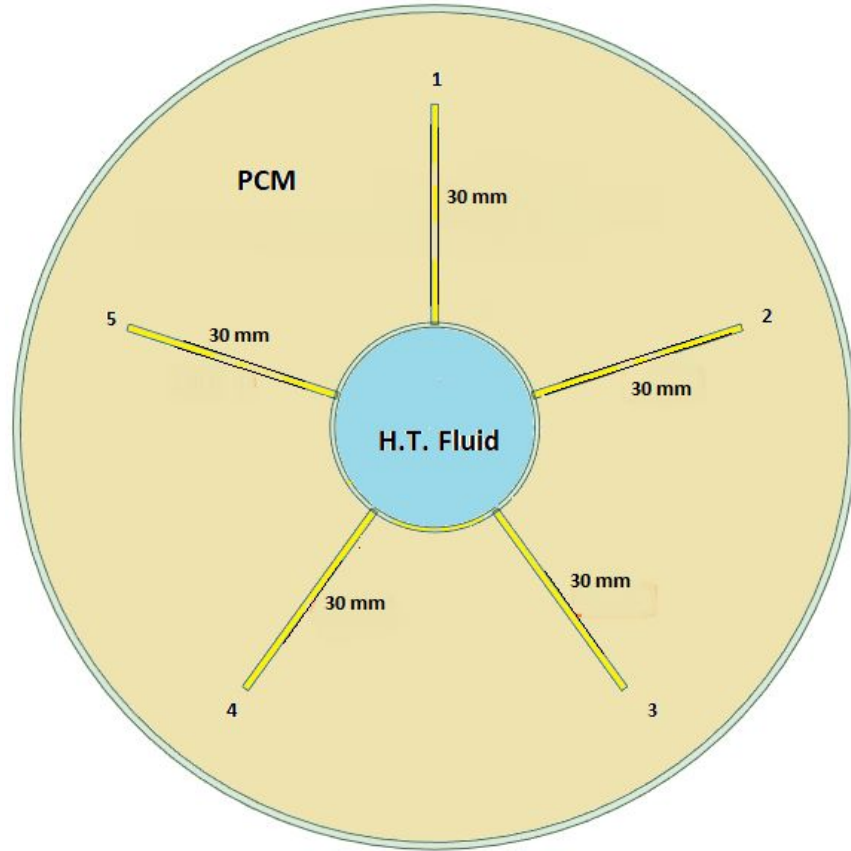
$$\rho C_p \frac{\partial T}{\partial t} = k \left( \frac{\delta^2 T}{\delta x^2} + \frac{\delta^2 T}{\delta y^2} + \frac{\delta^2 T}{\delta z^2} \right) + \frac{\partial}{\partial x}(S\rho L)(1)$$

Where,  $\rho$  is the density of PCM,  $C_p$  heat capacity of PCM,  $K$  thermal conductivity of PCM,  $S$  is liquid fraction and  $L$  latent heat of phase change. Enthalpy-porosity theory can be used to include the impact of phase-change materials in the energy equation as shown below: (Arosemena 2018)

$$\rho C_p \left( \frac{\partial T}{\partial t} + u \frac{\partial T}{\partial x} + v \frac{\partial T}{\partial y} + w \frac{\partial T}{\partial z} \right) = k \left( \frac{\delta^2 T}{\delta x^2} + \frac{\delta^2 T}{\delta y^2} + \frac{\delta^2 T}{\delta z^2} \right) + \frac{\partial}{\partial x}(S\rho L)(2)$$

where  $u$ ,  $v$  and  $w$  are the velocity components in  $x$ ,  $y$  and  $z$  direction. Solving these two equations analytically can be challenging, especially for complex geometries like heat exchangers. Instead, numerical methods are commonly employed, such as the finite element method, finite volume method, and finite difference method. These numerical techniques enable the simultaneous solution of the differential equations (D.E.) and energy equations (E.E) for the same phase change material (PCM). A combined approach is used, incorporating both equations and employing a penalty method to eliminate undesired terms over time, corresponding to the liquid state of the segment. Additionally, the momentum and continuity equations are utilized to account for natural convection, while the standard momentum, continuity, and energy equations are applied for the heat transfer fluid. Numerous software applications are available for solving numerical solutions, and one of the most renowned ones is Fluent, part of the ANSYS package. In this study, ANSYS 21 was utilized for numerical simulations.

#### Physical model:



Theoretical simulations were performed on three 3D models of a PCM heat exchanger to select the optimal design for melting and solidification processes. Each model featured a distinct fin length distribution while maintaining the same surface area and PCM volume. Figure (1) illustrates the cross-sections of these models.

Table (1): The Dimensions of Three Models

models	Fin length (mm)	Outer diameter				
	1	2	3	4	5	
A-1	30	30	30	30	30	113 mm
A-2	20	25	25	40	40	
A-3	30	25	25	35	35	

The three models were developed based on an understanding of natural convection in phase change material (PCM), drawing from previous studies. In these models, five fins were selected to achieve a balance between enhancement, reduced fin weight, and increased thermal storage capacity of the PCM heat exchanger (H.E.).

In the melting process, fresh molten PCM ascends to the top of the container, leading to an increase in the temperature of the upper half. Therefore, there is no need to increase the fin portion in the upper half. Conversely, during solidification, fresh cooled PCM descends to the bottom of the container, causing the temperature of the lower half to drop faster than that of the upper half. Therefore, adjusting the fin length distribution is crucial to achieve the optimal performance during both melting and solidification.

Considering these considerations, three designs were proposed:

1. The first design features uniform-length fins and serves as the reference model for comparison. Figure (1) A.
2. The second design, labeled A-2, has a greater fin portion in the lower half compared to the upper half of the container. Figure (1) B.
3. The third model, A-3, also has a larger fin portion in the lower half, but it is less than that of the A-2 model. Figure (1) C.

Three-dimensional simulation models of a horizontal tabular phase change material (PCM) H. E. with five longitudinal copper fins were created. The dimensions of the components are presented in Table (1), and the length of the heat exchanger is 500 meters, as illustrated in Figure (2).

### Hosted file

image7.emf available at <https://authorea.com/users/672730/articles/671678-the-optimum-fins-length-distribution-of-tabular-pcm-heat-exchanger>

Paraffin wax was selected as the phase change material (PCM) due to its high latent heat of melting, cost-effectiveness, and low melting temperature. The properties of the PCM are provided in Table (2).

Melting temperature [C]	46-61
Latent heat [J/Kg]	235512.5
Specific heat [J/Kg.K]	2460 Liquid/ 1456 solid
Thermal conductivity [W/m.k]	0.158 Liquid/ 0.259 solid
Thermal expansion coefficient [K-1]	0.000307
Density [Kg/m3]	7830.000307*(?-319)+1
Viscosity [Kg/m.s]	0.001*?xp(-4.25+1790?)

Water was employed as the heat transfer fluid because of its high thermal capacity and excellent thermal conductivity. The inner tube and fins are made of copper, while the outer tube is insulated.

The simulation conditions were set as follows: the heat transfer fluid (H.T.F.) temperature is 300 K for melting and 360 K for solidification. The mass flow rate is 0.25 kg/sec, and the initial temperatures are 360 K for melting and 300 K for solidification. The duration of the run is 3600 seconds for melting and 7200 seconds for solidification, reflecting the slower pace of the solidification process compared to melting.

The mesh size was meticulously chosen after numerous evaluation tests to attain the optimal balance between accuracy and time efficiency. It consists of 1,200,000 elements, with each time step test taking approximately 30 seconds. The time step, set at 1 second, was determined through time step evaluation tests during the mesh size selection process. The solution control parameters were adopted from previous studies for consistency.

### Result and discussion

The results were visualized in plots displaying the heat transfer rate ( $q$ ), the volume-averaged liquid fraction, and PCM temperature over time. These plots were complemented by visual observations of liquid fraction and temperature contours, providing valuable insights into the melting and solidification processes. They also highlight the significant role of natural convection in each phase.

#### Melting Process:

The simulation of the melting process was carried out over a period of 3600 seconds for all three models, allowing for a comparative analysis. The results are presented in Figure (3):

The diagram under discussion Figure (4), which chronicles the changes in liquid fraction over the course of the melting process, is commonly known as a "Liquid Fraction Time-Lapse Diagram." This visual representation delineates the evolving behavior of the phase change material (PCM) as it undergoes the melting process through distinct phases.

In the initial stage, the PCM adjacent to the fin walls gradually transforms into a liquid state, primarily facilitated by conduction. As time elapses, the thickness of the liquefied layer steadily increases. Once this layer attains a sufficient thickness, the onset of natural convection currents marks the commencement of the second stage.

Throughout the second stage, four discrete regions of melted PCM manifest themselves. Region (1) originates from fin (1), while region (2) results from the melted PCM arising from fin (2) and the upper surface of fin (4). Region (3) is generated from the melted PCM originating from fin (3) and the upper surface of fin (5), and region (4) emerges from the lower surface of fin (4) and fin (5). Natural convection becomes increasingly influential during this phase, driven by the broadening expanse of the melted PCM region and the expanding interface between the melted and solid PCM.

In the ultimate stage, regions (1), (2), and (3) amalgamate to create a unified melted PCM domain in the upper half of the cylinder. In this phase, the pace of the melting process decelerates as the influence of natural convection diminishes. This decline is attributable to the diminishing boundary between the melted and solid PCM, which results in a flatter, semi-horizontal line. Over time, this line contracts until complete melting is achieved.

This "Liquid Fraction Time-Lapse Diagram" offers a comprehensive visual narrative of the melting process and the evolving role of natural convection across different phases.

Figure (4) presents the evolution of the liquid PCM fraction over time. The results demonstrate a consistent increase in the liquid fraction. In the first and second stages, as discussed earlier, the liquid fraction exhibits a linear increase over time. However, as we enter stage (3), this increase becomes slightly less pronounced compared to the initial stages. Notably, the deceleration effect is more prominent in the A-1 model, attributable to the greater distance of the lower fins from the bottom of the heat exchanger (H.E.). Across the first two stages, the liquid fraction in model A-1 surpasses that of the other two models. Yet, in the third stage, the liquid fraction in A-1 lags the other two models. Models A-2 and A-3 exhibit nearly identical liquid fractions, with A-2 displaying a marginally higher liquid fraction during the third stage for the same time frame. In summary, the liquid fraction graph indicates that, overall, models A-2 and A-3 outperform A-1.

Model Time(Sec)	A-1	A-2	A-3	
515				
1030				
1545				
2060				
2575				
3090				
3600				
Figure (3): Time Frames of Liquid Fraction Contours During the Melting Process.	Figure (3): Time Frames of Liquid Fraction Contours During the Melting Process.	Figure (3): Time Frames of Liquid Fraction Contours During the Melting Process.	Figure (3): Time Frames of Liquid Fraction Contours During the Melting Process.	Figure (3): Time Frames of Liquid Fraction Contours During the Melting Process.

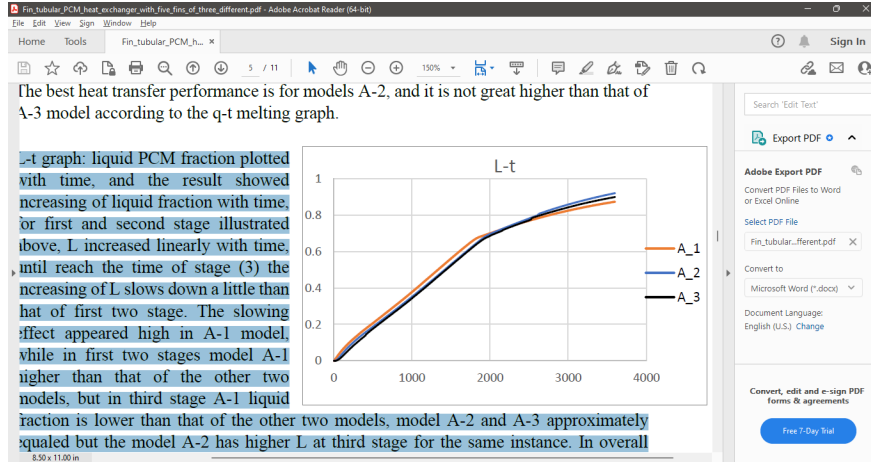


Figure 5 illustrates the time-lapse of melting temperature. Observing the temperature contours over time, it's evident that the temperature distribution closely mirrors the behavior of the liquid fraction. In the initial stage, the temperature in the boundary layer gradually rises until it reaches the PCM's liquidous temperature, signifying the onset of PCM melting. Subsequently, the temperature experiences a gradual increase over time.

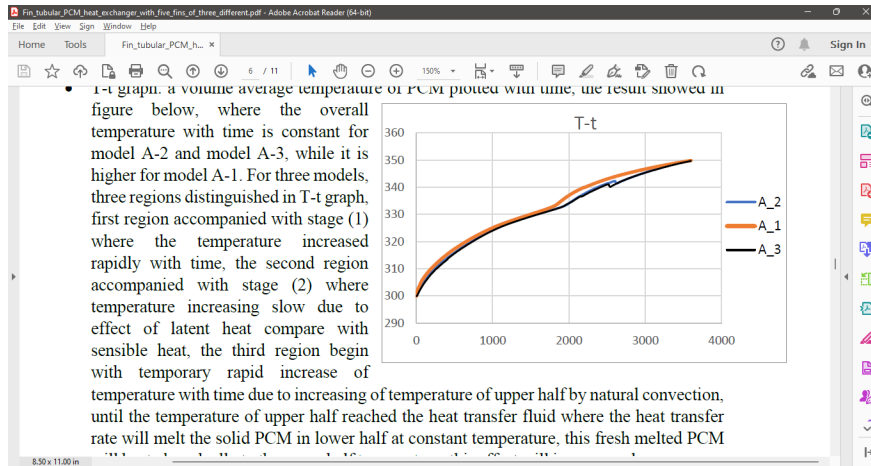
In the second stage, the temperature of the melting PCM steadily rose until it entered the third stage, marked by a notable increase until it reached the heat transfer fluid (H.T.F.) temperature. During this temperature increase, the primary mode of heat transfer to the PCM was sensible heat in the upper half, with a minor contribution of latent heat in the lower half. As the upper half reached the H.T.F. temperature, natural convection reached its minimal level. Subsequently, heat transfer predominantly occurred through conduction as latent heat to the lower solid PCM.

These stages appeared in three models, although at different times, as illustrated in figures 3 and 5. Whereas model A-2 melts faster than model A-3, model A-1 melts the slowest. The merging of regions (1, 2, and 3) is slower in models A-2 and A-3 than in model A-1 because the side fins (fins 2 and 5) are shorter, and those fins contributed to generation region (2 and 3), so the merging will be delayed with region (1), as discussed in heat transfer rate graphs. While region (4) is created faster in models A-2 and A-3 and contains more melted PCM, this is due to longer lower fins (fin number 3 and 4) that contribute to region (4) generation.

Figure (6) displays the results of the volume-averaged temperature of the PCM over time. The temperature behavior over time reveals distinct patterns among the three models. Model A-2 and Model A-3 maintain a consistent temperature over time, whereas Model A-1 exhibits a higher overall temperature. The temperature graph exhibits three distinct regions for all three models. The first region corresponds to stage (1), marked by a rapid temperature increase over time. The second region aligns with stage (2), where the temperature increase slows due to the influence of latent heat as opposed to sensible heat. In the third region, a temporary, rapid temperature increase over time is observed. This increase results from the rising temperature of the upper half due to natural convection until it reaches the temperature of the heat transfer fluid. At this point, the heat transfer rate initiates the melting of the solid PCM in the lower half, maintaining a constant temperature. The fresh melted PCM gradually heats to match the temperature of the upper half, contributing to a gradual increase in the volume-averaged temperature over time.

Model Time(Sec)	A-1	A-2	A-3
515			
1030			
1545			

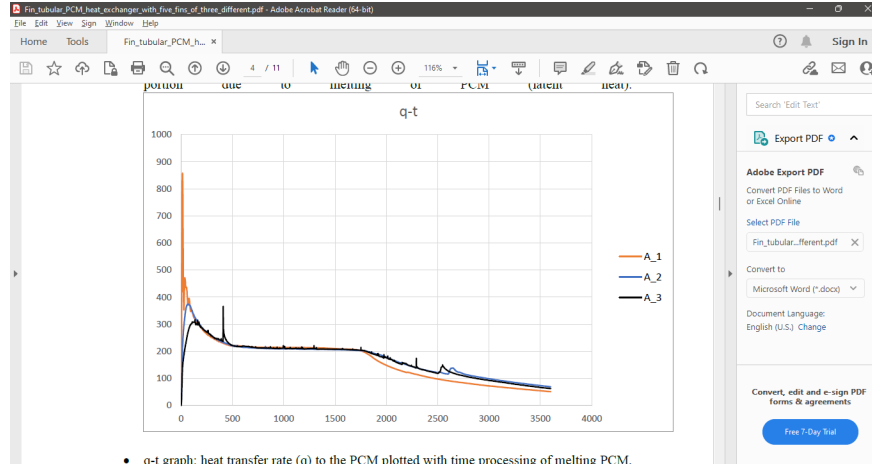
Model Time(Sec)	A-1	A-2	A-3	
2060				
2575				
3090				
3600				
Figure (5): Time Frames of Temperature Contours During the Melting Process.	Figure (5): Time Frames of Temperature Contours During the Melting Process.	Figure (5): Time Frames of Temperature Contours During the Melting Process.	Figure (5): Time Frames of Temperature Contours During the Melting Process.	Figure (5): Time Frames of Temperature Contours During the Melting Process.



For the melting process, the heat transfer rate ( $q$ ) to the phase change material (PCM) is depicted over time in Figure (7), providing a comparison of heat transfer rates among the three models. In all three models, the heat transfer rate initiates an upward trend as the adjusting layer of PCM begins to melt and contacts the fin surfaces. This trend continues until it reaches the peak heat transfer rate. At this point, the width of the melted PCM layer expands, leading to a reduction in conduction heat transfer. Consequently, the heat transfer rate experiences a rapid decline from its peak. It eventually reaches a stage where four distinct regions of natural convection, as discussed in the previous section, become apparent. In this stage, the increase in natural convection counters the decrease in conduction, resulting in the heat transfer rate becoming nearly constant over time. As stage three commences, marked by the restriction of natural convection and the reduction of the front line of melting due to the merging of upper regions of melted PCM, the heat transfer rate gradually decreases until full melting is achieved.

The optimal heat transfer performance is associated with a higher heat transfer rate over time across all stages. The highest peak in heat transfer rate is observed in the A-1 model, characterized by equal fin lengths. This peak is attributed to the uniform melting process at the fin surfaces. In contrast, the A-2 and A-3 models exhibit lower peaks due to the varying melting rates among the fins. Fins 1, 2, and 3 melt more rapidly than fins 4 and 5, with the faster-melting fins reaching stage one before the longer fins reach full melting. However, it's worth noting that the peak value doesn't significantly impact the overall heat performance. During stages 1 and 2, the heat transfer rate remains nearly constant for all models due to the consistent surface area of the fins, leading to an equal melting front line for all. Stage 2 is relatively shorter in duration for these models, primarily because the upper melted PCM region merges earlier, as depicted in Figure (4). In stage 3, the longer bottom fins (4 and 5) enhance heat transfer to the PCM in

the form of latent or sensible heat. This heated or melted PCM rises to the top until the upper half reaches the temperature of the heat transfer fluid. At this point, heat transfer to the melted PCM at the bottom occurs through conduction, highlighting the significance of fin length at the solid bottom. Therefore, the heat transfer rate for both A-2 and A-3 models in stage 3 is approximately equal, as they possess similar bottom fin lengths. The A-2 model exhibits the best heat transfer performance, although it is only marginally higher than that of the A-3 model, as indicated by the heat transfer rate graph.



### Solidification :

For simulated the solidification process, a time of 7200 seconds was considered for the investigation of the three models, which are to be compared. The results obtained are as follows:”:

Figure (8) presents the liquid fraction contour during the solidification process for the three models. It depicts the growth of the solid PCM layer on the fin surfaces over time and the separation of fully melted PCM to the top of the heat exchanger. The time lapse of the liquid fraction contour reveals distinct stages. In the first stage, the melted PCM adjusts to the fin surfaces, and the cooled melted PCM settles down. The next stage involves the generation of fully solid PCM at the fin surfaces. During this stage, fully melted PCM floats in the upper quarter, while the remainder of the PCM is partially melted. In the later stages of solidification, the width of the fully solid layer increases, and the upper fully melted PCM disappears as the process reaches full solidification. It’s noteworthy that the upper fully melted quarter in the A-1 model disappears sooner than in the A-2 model, and the upper melted PCM in A-2 also vanishes earlier than in the A-3 model. This variation is explained by the top fin’s length (1), which provides superior conductivity than the shorter fins.

Figure (9) shows the liquid fraction with time, indicating three separate zones. The first region is distinguished by a short, constant liquid fraction, which is followed by a second region in which the liquid fraction rapidly drops over time. These two regions correspond to the first stage of the liquid fraction contour. The third region begins at approximately 1000 seconds, displaying a slow, gradual decrease in liquid fraction over time.

When examining the liquid fraction graph, it’s evident that Model A-1 consistently maintains a lower liquid fraction at each time point, while Model A-3 exhibits slightly higher liquid fractions. Model A-2, on the other hand, displays the highest liquid fraction. Model A-1 and A-3 are roughly equal, or there are only minor differences between them, primarily due to the same top fin length, which facilitates cooling in the upper, hotter half.

Model Time(Sec)	A-1	A-2	A-3	
1030				
2060				
3090				
4120				
5150				
6180				
7200				
Figure (8): Time Frames of Liquid Fraction Contours During the Solidification Process.	Figure (8): Time Frames of Liquid Fraction Contours During the Solidification Process.	Figure (8): Time Frames of Liquid Fraction Contours During the Solidification Process.	Figure (8): Time Frames of Liquid Fraction Contours During the Solidification Process.	Figure (8): Time Frames of Liquid Fraction Contours During the Solidification Process.

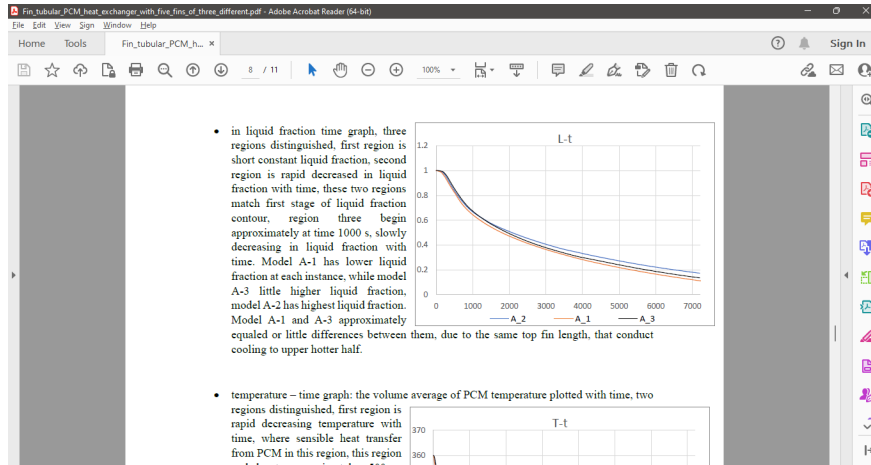


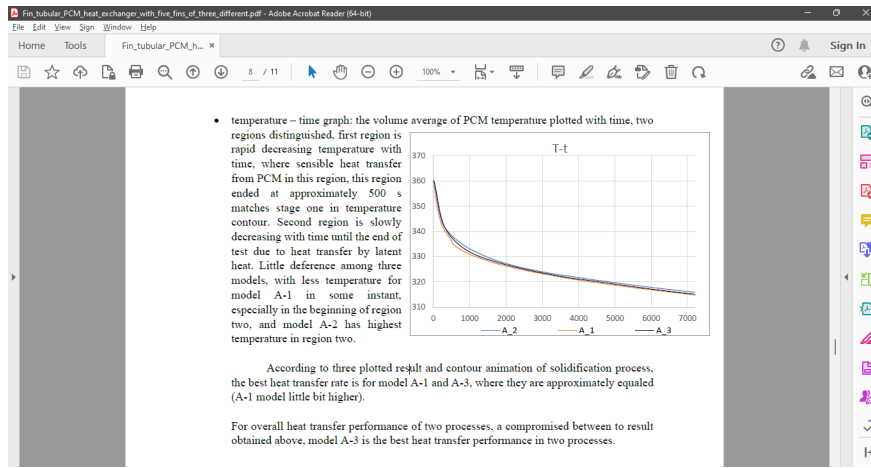
Figure (10) displays the temperature contour over time during the solidification process. Initially, the temperature of the melted PCM decreases, causing the hotter PCM to rise to the top. The overall temperature of the melted PCM reaches the solidus temperature, achieving a uniform temperature distribution at around 500 seconds for all three models. At this stage, a solid layer forms on the fin surface. The temperature of this layer decreases to match the heat transfer fluid temperature during solidification, and the layer width gradually increases until full solidification is achieved.

Figure (11) displays the temperature versus time graph, showing the volume averaged PCM temperature over time. Two distinct regions are observed. The first region is characterized by a rapid decrease in temperature over time, primarily driven by sensible heat transfer from the PCM. This region concludes at around 500 seconds, corresponding to stage one in the temperature contour. The second region exhibits a gradual decrease in temperature over time due to heat transfer by latent heat, continuing until the end of the test.

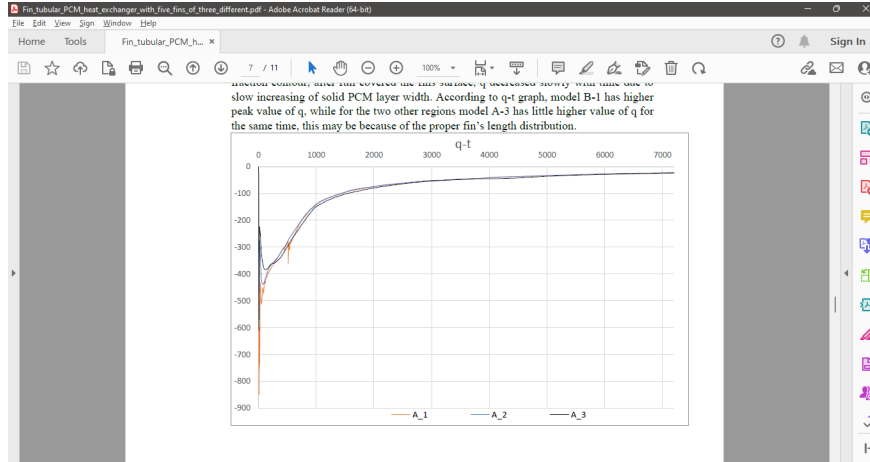
There are slight differences among the three models, with Model A-1 having slightly lower temperatures at certain instances, particularly at the beginning of region two. Model A-2, on the other hand, features the highest temperatures in region two.

Model Time(Sec)	A-1	A-2	A-3
1030			

Model Time(Sec)	A-1	A-2	A-3	
2060				
3090				
4120				
5150				
6180				
7200				
Figure (10): Time Frames of Temperature Contours During the Solidification Process.	Figure (10): Time Frames of Temperature Contours During the Solidification Process.	Figure (10): Time Frames of Temperature Contours During the Solidification Process.	Figure (10): Time Frames of Temperature Contours During the Solidification Process.	Figure (10): Time Frames of Temperature Contours During the Solidification Process.



In Figure (12), which represents the heat transfer rate during the solidification process over time, three distinct regions are observed. The first region witnesses a short, rapid increase in the heat transfer rate. This increase is attributed to the solidification of the adjusting PCM to the fin surfaces. The second region is characterized by a fast decrease in the heat transfer rate over time, as the solid PCM layer is generated, ultimately covering the fin surfaces. These first two regions correspond to stage one in the liquid fraction contour. Once the fin surfaces are fully covered by the solid PCM layer, the heat transfer rate decreases gradually over time due to the slow expansion of the solid PCM layer width.



Analyzing the heat transfer rate graph, Model A-1 exhibits a higher peak value for the heat transfer rate, while in the other two regions, Model A-3 displays slightly higher values of heat transfer rate for the same time frame. This difference may be attributed to the appropriate distribution of fin lengths.

In summary, considering the results from the plotted data and contour over time of the melting and solidification processes, the best heat transfer rate is achieved by Models A-1 and A-3, with Model A-1 having a slight edge. In overall performance across both processes, Model A-3 demonstrates the optimum heat transfer performance, showcasing significant improvement in melting and a good performance in solidification.

### Conclusion :

It is clear from the research on the optimal fin length distribution for a tubular PCM heat exchanger that the choice of fin design has a substantial impact on improving the efficiency of heat transfer during both melting and solidification processes. Numerical simulations of the three fin length distribution designs were used to thoroughly assess them, and the findings have given us important information about the best design. The study's main conclusions can be summed up as follows:

1. Optimum Design: Model A-3, one of the three models under investigation, stood out as the best layout. The bottom fins in this style are longer but the top fins are kept at their original length with shorter side fins. The best heat transfer efficiency for both melting and solidification processes was discovered to be offered by it.
2. Influence of Lower Fins: The study shows that by encouraging effective heat transport, lengthening the bottom fins has a favorable effect on melting. But it was also noted that this modification slows the solidification process.
3. Significance of Upper and Lower Fins: The study emphasizes the importance of the upper and lower fins in a five-longitudinal-fin tubular Phase Change Material heat exchanger over the side fins. As a result, the design of these fins is critical for achieving optimal heat transfer performance.

Finally, selecting the proper fin length distribution design in a tubular PCM heat exchanger is crucial for enhancing heat transfer efficiency throughout the melting and solidification processes. Model A-3 has been selected as the most effective alternative for improving heat transfer in both stages due to its fin arrangement. These findings offer useful insights for the design and optimization of PCM heat exchangers, with implications for a wide range of heat storage and management applications. More research and practical use of such designs may result in more efficient and sustainable thermal energy systems.

### References:

- Al-Ebadi, H. and M. Abdullah (2022). "Numerical Study of Thermal Conductivity Effect on The Performance of Thermal Energy Storage." *Journal of Engineering* **28** (10): 57-77.
- Al-Mudhafar, A. H. N., A. F. Nowakowski and F. C. G. A. Nicolleau (2018). "Thermal performance enhancement of energy storage systems via phase change materials utilising an innovative webbed tube heat exchanger." *Energy Procedia* **151** : 57-61.
- Ali N. Abdul Ghafoor, M. A. M. (2020). "Numerical Study of A Thermal Energy Storage System with Different Shapes Inner Tubes." *Journal of Mechanics of Continua and Mathematical Sciences* **15** (4): 21-35.
- Aneke, M. and M. Wang (2016). "Energy storage technologies and real life applications – A state of the art review." *Applied Energy* **179** : 350-377.
- Arosemena, A. (2018). Numerical Model of Melting Problems.
- Aydin, O., A. Mete, M. Y. Yazici and M. Akgun (2018). "Enhancing storage performance in a tube-in shell storage unit by attaching a conducting fin to the bottom of the tube." *Isı Bilimi ve Tekniği Dergisi* **38** (2): 1-13.
- Azim, M. and A. K. Gupta (2020). *Melting and Thermal Behavior of Phase Change Materials Around an Asymmetrically Confined Circular Cylinder* . Proceedings of the International Conference on Advances in Chemical Engineering (AdChE).
- Deng, S., C. Nie, G. Wei and W.-B. Ye (2019). "Improving the melting performance of a horizontal shell-tube latent-heat thermal energy storage unit using local enhanced finned tube." *Energy and Buildings* **183** : 161-173.
- Fathi, M. I. and M. A. Mussa (2021). "Experimental study on the effect of tube rotation on performance of horizontal shell and tube latent heat energy storage." *Journal of Energy Storage* **39** .
- Fathi, M. I. and M. A. Mussa (2021). "Numerical Study for the Tube Rotation Effect on Melting Process in Shell and Tube Latent Heat Energy Storage LHES System." *Journal of Engineering* **27** (11): 75-96.
- Fathi, M. I. and M. A. Mussa (2023). "The effect of whole system rotation on the thermal performance of a phase change energy storage." *Journal of Energy Storage* **68** : 107732.
- Huang, B., S. Yang, J. Wang and P. D. Lund (2022). "Optimizing the shape of PCM container to enhance the melting process." *Oxford Open Energy* **1** : oiab006.
- Joudi, K. A. and A. K. Taha (2023). "Simulation of Heat Storage and Heat Regeneration in Phase Change Material." *Journal of Engineering* **18** (09): 1055-1072.
- Kamkari, B. and D. Groulx (2018). "Experimental investigation of melting behaviour of phase change material in finned rectangular enclosures under different inclination angles." *Experimental Thermal and Fluid Science* **97** : 94-108.
- Mahood, H. B., M. S. Mahdi, A. A. Monjezi, A. A. Khadom and A. N. Campbell (2020). "Numerical investigation on the effect of fin design on the melting of phase change material in a horizontal shell and tube thermal energy storage." *Journal of Energy Storage* **29** : 101331.
- Mehta, D., S. Chaudhari, M. Rathod and J. Banerjee (2017). *Effect of orientation of shell and tube latent heat storage unit on melting phenomena of phase change material* . Proceedings of the 24th National and 2nd International ISHMT-ASTFE Heat and Mass Transfer Conference (IHMTTC-2017), Begel House Inc.
- Mehta, D. S., B. Vaghela, M. K. Rathod and J. Banerjee (2020). "Enrichment of heat transfer in a latent heat storage unit using longitudinal fins." *Heat Transfer* **49** (5): 2659-2685.
- Motevali, A., M. Hasandust Rostami, G. Najafi and W.-M. Yan (2021) "Evaluation and Improvement of PCM Melting in Double Tube Heat Exchangers Using Different Combinations of Nanoparticles and PCM (The Case of Renewable Energy Systems)." *Sustainability* **13** DOI: 10.3390/su131910675.

- Nabhan, B. J. (2015). "Using nanoparticles for enhance thermal conductivity of latent heat thermal energy storage." *Journal of Engineering* **21** (6): 37-51.
- Nagar, S. and P. K. Singh (2021). "A short review on the Industrial applications of phase change materials." *IOP Conference Series: Materials Science and Engineering* **1116** (1): 012006.
- Pizzolato, A., A. Sharma, K. Maute, A. Sciacovelli and V. Verda (2017). "Design of effective fins for fast PCM melting and solidification in shell-and-tube latent heat thermal energy storage through topology optimization." *Applied Energy* **208** : 210-227.
- Rudonja, N. R., M. S. Komatina, G. S. Živković and D. L. Antonijević (2016). "Heat transfer enhancement through PCM thermal storage by use of copper fins." *Thermal Science* **20** : S251-S259.
- Sadiq, H. H. and M. A. Mussa (2022). "Experimental Study of Thermal Conductivity Effect on the Performance of Thermal Energy Storage." *Jordan Journal of Mechanical & Industrial Engineering* **16** (4).
- Shahid Afridi, M., A. Anthony, P. Sundaram and S. Babu (2018). "Experimental comparison of longitudinal and annular fins using PCM for Thermal energy storage." *IOP Conference Series: Materials Science and Engineering* **402** (1): 012179.
- Soltani, H., M. Soltani, H. Karimi and J. Nathwani (2021). "Heat transfer enhancement in latent heat thermal energy storage unit using a combination of fins and rotational mechanisms." *International Journal of Heat and Mass Transfer* **179** : 121667.